

Experimental forecasts of El Niño

Mark A. Cane, Stephen E. Zebiak & Sean C. Dolan

Lamont-Doherty Geological Observatory of Columbia University, Palisades, New York 10964, USA

Experimental forecasts of El Niño events occurring since 1970, made with a deterministic model of the coupled ocean-atmosphere system, indicate that El Niño is generally predictable one or two years ahead. A forecast for 1986 is also presented.

THE devastating climatic events of 1982–83 were the most recent extreme phase of the irregular cycle of atmospheric and oceanographic changes known collectively as El Niño and the Southern Oscillation (ENSO)^{1–5}. If forecasts could provide sufficient warning of an impending episode, appropriate planning could reduce human suffering and economic loss^{6,7}. In 1982 the state of information gathering and forecasting activities was clearly inadequate: the event was well under way before it was recognized. Statistical procedures reported more recently^{8,9} could have forecast it in the spring of 1982, a few months in advance of the peak warming.

Forecasts of El Niño at longer lead times could be impossible in principle. Perhaps the intrinsic behaviour of the coupled ocean–atmosphere system is such that states which initially differ by a small amount diverge very rapidly. If so, it would be impossible to observe initial conditions with sufficient precision to determine the subsequent evolution over many months. Even if skilful forecasts at longer range are possible in principle, they may be unattainable in practice because of inadequate models or the limitations of available data.

While it leaves many questions unanswered, the work reported here offers grounds for optimism. We have used a deterministic numerical model of the coupled ocean and atmosphere in the tropical Pacific region to make forecasts of all the El Niño events since 1970. The results indicate that the large-scale warmings associated with these events could have been predicted a year or more in advance.

The numerical forecasting model^{10,11} is a coupled model for the evolution of the ocean and atmosphere in the tropical Pacific region. Only deviations from the mean are calculated explicitly; mean conditions are specified from monthly climatological data. No statistical procedures are used in the forecasts. Model variables evolve deterministically, according to the physical laws governing the atmosphere and oceans. The model was originally developed for abstract studies of large-scale ocean–atmosphere interactions in the tropics and is far simpler than the numerical models used operationally for weather prediction. Nevertheless, it reproduces much of the characteristic spatial and temporal structure of observed El Niño events, including their recurrence at irregular intervals with an average period of 3–4 yr (refs 10, 11).

In part, the simplifications were designed to serve a didactic purpose: insofar as the model simulations of ENSO are judged to be correct, one may conclude that the omitted processes are not essential for the existence of the ENSO cycle. When the model is to be used for forecasting, however, verisimilitude is clearly desirable and the simplifications are a handicap. The model's predictive skill is probably decreased by the absence of the 30–60-day waves so prevalent in the tropics¹², as well as by the lack of any variability generated in mid-latitudes. The model exhibits too little variability in the western equatorial Pacific and overstates easterly wind anomalies in the east. It cannot reproduce episodes of strong cold anomalies. All of these flaws (and others) reduce the realism of its ENSO simulations.

On the basis of model results, we have suggested a theory for the ENSO cycle^{10,11} along lines proposed by Bjerknes¹³ almost two decades ago. Many investigators since Bjerknes have substantially advanced our understanding of the tropical atmos-

phere and oceans, allowing his original framework to be bolstered and elaborated. Our theory and model design draw on this collective progress^{1,14}, only a brief sketch of which is possible here.

Ocean–atmosphere interaction

Work on equatorial ocean dynamics following the pioneering sea-level studies of Wyrtki^{15,16} established that changes in the eastern equatorial Pacific could be caused by remote wind changes to the west, with the signal propagating through the ocean along the equatorial wave guide¹⁷. Others explored the ways in which ocean dynamics^{13,18–20}, not surface heating anomalies^{4,13,21}, accounted for observed anomalies in sea surface temperature (SST). Experiments with atmospheric general circulation models^{22–24} showed that tropical Pacific SST anomalies could cause the meteorological changes characteristic of ENSO; other studies showed that simple models could largely account for the tropical aspect of the anomaly pattern^{4,25–28}.

If the winds alter the SST pattern, which alters the winds, then a coupled ocean–atmosphere model is clearly required. Although highly idealized, the models described in the literature^{29–33} provide considerable insight into the mechanics of growing and oscillating modes of the coupled system. (This work has been reviewed by McCreary³⁴).

In our model, the atmosphere and ocean both have an active role in ENSO: it is an oscillation of the coupled system. Its consequences are global, but the interactions vital to its existence all occur in the tropical Pacific region.

In the normal state, the tropical Pacific is warmer in the west and colder in the east; a centre of tropical rainfall overlies the pool of very warm water in the far western Pacific. The easterly trade winds blowing towards this atmospheric heating region drive warm surface waters to the west, while drawing colder sub-surface waters upward at the east. Thus, the temperature contrast responsible for the atmospheric circulation is maintained by that circulation—a positive feedback.

If the eastern ocean becomes warmer, then the rainfall spreads eastward with the warm water, and the surface winds slacken. As a result, some of the warm western water moves eastward and less cold water is drawn upwards; hence, the east becomes warmer still. Again, there is a positive feedback, leading to more westerly winds, warmer SSTs and a deeper thermocline in the east. This is an El Niño event.

Bjerknes¹³ discussed both of these 'chain reactions' but could not explain why there were transitions from one phase to the other in an endless cycle. The key idea in our theory requires going beyond the vertical plane along the Equator and considering the north–south circulation in the ocean^{4,18,29}. Approaching the peak of an El Niño event, water moves not only from west to east, but also poleward³⁵, emptying the reservoir of warm water at the Equator.

In the aftermath of the event, the heat loss results in colder than normal eastern Pacific SSTs and, consequently, stronger than normal easterlies—an enhanced version of the non-El Niño state. The transition back to the El Niño state cannot take place until enough warm water flows back from higher latitudes to refill the equatorial heat reservoir. Episodes of weak easterlies are frequent, but until the reservoir is refilled there is not enough

warm water available to sustain the 'chain reaction' that generates an El Niño event.

Our focus on the heat content of the equatorial band arose from theoretical considerations and numerical model results. There is also observational evidence supporting these ideas. On the basis of tide gauge data, Wyrtki³⁶ has independently advanced a similar hypothesis.

The time it takes to restore the equatorial heat content depends on the strength of the coupling between atmosphere and ocean¹⁰. The phenomenological 'coupling strength' comprises a number of factors, such as the sharpness of the thermocline, advective speeds, oceanic temperature gradients, dissipation rates, oceanic wave speeds and the sensitivity of the surface wind to SST contrasts. All of these vary seasonally and spatially, in addition to changing with the state of the ocean-atmosphere system. In addition, the flow of warm water back to the Equator is affected by higher-frequency events such as the 30–60-day waves¹² in the western Pacific.

The irregularity of the interval between El Niño events reflects the variability of this refill time; it is this variability which makes the prediction of El Niño difficult. It is not known whether it is more a result of high-frequency noise³⁷ or of the nonlinearities intrinsic to the ENSO cycle³⁸. Although either implies that the ENSO cycle cannot be predicted arbitrarily far ahead, neither precludes prediction at useful lead times.

The ENSO scenario outlined here has further implications for the prospects of forecasting an El Niño event. As the essential interactions take place in the tropical Pacific, data from that region alone should be sufficient for forecasting. Also, our model implies that the future evolution of the ENSO cycle could not be predicted without knowledge of the upper-ocean heat content. The radiative relaxation time of the atmosphere is ~1 month, and the thermal damping time of the ocean surface layer is at most a few months (4 months in the model). Evidence that El Niño can be predicted at significantly longer lead times implies an active role for the sub-surface ocean, which has substantially greater thermal inertia.

In the model, the sub-surface thermal structure reduces to a single variable, the anomaly in the heat content of the upper ocean, or, equivalently, the thermocline depth anomaly. (A recent empirical study highlights the same variable³⁹.) The analysis above implies that this variable is an essential initial input for forecasting. As available observations are insufficient to specify a complete field of thermocline depth anomalies, the following procedure was adopted. A field of monthly mean surface wind stress anomalies was derived from ship observations over the tropical Pacific⁴⁰; a 1–2–1 filter in time, longitude and latitude was then applied to the winds analysed. The anomalies used are the deviations from the average of the same calendar month over the previous 4 years; for example, the May 1985 anomaly is the deviation from the mean of May 1982, 1983, 1984 and 1985.

The period up to the forecast initial time was simulated by forcing the ocean component of the coupled model with wind-stress anomaly fields specified for each month starting with January 1964. The computed SST anomalies were then used to run the atmospheric component of the model. The calculated anomalies in thermocline depth, currents, SST and surface winds were then used as initial conditions for a forecast with the coupled model. Note that the initial SST and wind fields are calculated to be compatible with the initial thermocline displacements within the model framework; they need not agree with observed SST or wind fields. The coupled model runs evolve from the initial conditions as in a true forecast model: no new data are introduced after the initial time.

Forecast results

Figure 1 compares a map of observed SST anomalies during the peak period, January 1983, with that from the forecast initiated in January 1981. The result is typical of the more

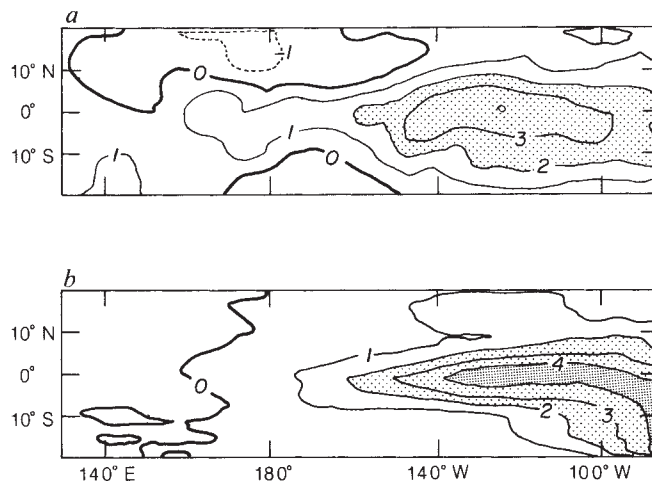


Fig. 1 Sea surface temperature (SST) anomalies (°C) in January 1983. *a*, Observed, based on the analysis of the Climate Analysis Center (CAC) of NOAA. *b*, Predicted by the model forecast initiated in January 1981, 2 years earlier.

successful forecasts. As in earlier work¹⁰, including cases with the same ocean model driven by observed winds²⁰, the gross character of the eastern Pacific El Niño SST anomaly is reproduced, although its meridional and westward extent is underestimated.

Forecasts were initiated in the periods preceding each of the El Niño events that have occurred since 1970; that is, the events of 1972, 1976 and 1982. An additional set was made for the 'non-event' of 1979. No forecasts were attempted in the years before 1970 because the wind analyses available for these earlier years are of distinctly lower quality. In each period there are six forecasts spaced 3 months apart, with the sequence ending in January of the nominal year. For example, for 1972 forecasts were initiated from October 1970, January, April, July and October, 1971 and January 1972.

The forecast results are summarized in terms of the SST anomaly averaged over the eastern equatorial Pacific area called NINO3 (5° S to 5° N; 90° W to 150° W). The NINO3 index was devised by the Climate Analysis Center of NOAA (National Oceanic and Atmospheric Administration) because a warming in this region strongly influences the global atmosphere². It is probably the best single indicator of an ENSO episode likely to affect global climate.

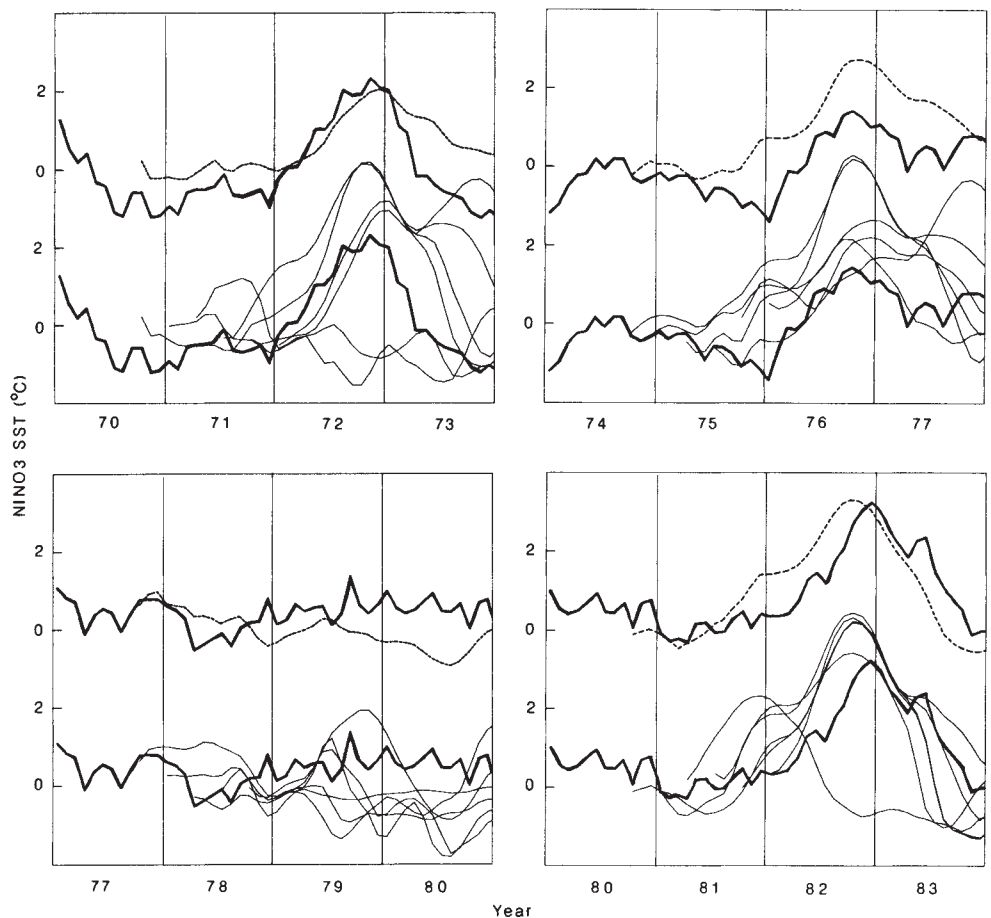
Figure 2 shows that the model generally succeeds in predicting warmings in those years when they were observed to occur, and

Table 1 Summary of forecast results for past years

Start month	No. right	No. of cases	Chance by coin flips
1-yr forecasts			
October	7	8	0.04
January	8	8	0.004
April	1	4	0.94
July	4	4	0.06
Total	20	24	0.0008
2-yr forecasts			
October	3	4	0.31
January	3	4	0.31
Total	6	8	0.14

Results correspond to the 24 forecasts of Fig. 2. For January, '1-yr forecasts' refers to the same calendar year; for all other start months, to the next calendar year. The last column shows the probability of correctly predicting at least as many cases as the model did by flipping a coin.

Fig. 2 SST anomalies ($^{\circ}\text{C}$) averaged over the eastern equatorial Pacific NINO3 region (90°W to 150°W , 5°S to 5°N) for four periods centred on 1972, 1976, 1979 and 1982. Heavy curves, observed values as reported by CAC/NOAA (note repetition of vertical scale). Light curves, values from six forecasts initiated at 3-month intervals from the October two years ahead to the January of the nominal year. Dashed curve, average of the six forecasts (the consensus forecast).



in predicting their absence when they did not occur. As with the observed events, the peaks in the NINO3 index are always forecast to take place at the end of the calendar year. The individual forecasts tend to give too strong an event, especially for the 1976 El Niño. The rise in temperature during 1976 is well predicted, but five of the six forecasts begin the year at least 2°C too warm. They entirely missed the 1975 cooling trend, which culminated in the coldest NINO3 SST in the entire data record. This failure is present even when the model is forced by observed winds, as in the run creating initial conditions (see, for example, the initial SST for the January 1976 forecast in Fig. 2). On the other hand, the model never predicts an El Niño for 1975, although at the time observers saw enough precursors of an event early in the year to announce an El Niño watch.

It is important to know whether the model's ability to predict whether an El Niño will occur is significantly better than chance. Because the distribution of states in the tropical Pacific is strongly bimodal¹, it is straightforward to distinguish El Niño events from non-events. In terms of NINO3 SST we will say there is an El Niño if there is a rise of at least 2°C within 12 months, leading to an anomaly of at least $+1.0^{\circ}\text{C}$ for at least 3 months. These criteria are derived from the observed events; the set of forecasts would score similarly for any other criteria able to separate observed events from non-events.

According to the above criteria, 19 of the 24 forecasts are correct. (The forecasts would be judged to be less successful if more detailed agreement with observation were demanded.) January 1971, April 1971, October 1975 and April 1981 fail to predict the upcoming event, and April 1978 falsely predicts an El Niño in 1979. Of the five failures, three are from April starts. In the spring the Intertropical Convergence Zone is closest to the Equator and the SST in the east is warmest. As a result the coupling between model atmosphere and ocean is such that noise in the initial state is easily amplified, leading to poor results. The real ocean-atmosphere system is also least predict-

able in the spring: it is the time when the Southern Oscillation index shows the smallest correlation with its future value⁴¹.

Meteorological forecasts are typically evaluated relative to climatology or persistence, but either overestimates the predictive skill for infrequent events like El Niño. Table 1 offers another standard: the random guess. It may seem artificially favourable to compare to a guessing strategy which makes no apparent use of the known 3-4-yr quasi-periodicity of the ENSO cycle²; however, we have forecast only for periods 3 or 4 years apart, when events are seemingly due. Hence the occurrence or non-occurrence of an event in any of the years in our sample is roughly equally likely, so that flipping a coin is a reasonable guessing strategy.

In order to establish a rigorous confidence level, the number of independent forecasts must be known. A precise determination of independence would require many more model runs, but estimates adequate for present purposes can be readily made. We treat forecasts that are 3 months apart as independent, based on the observation that qualitative behaviour (such as incorrect forecasts or maintaining high SST in the year after an event) rarely persists longer. Doing this probably overestimates the confidence level. At the other extreme, a very conservative estimate is obtained by assuming that the forecasts within each set are highly correlated. Then there are only four independent forecasts, each given by the majority of the six within each set. As all four are correct, there is 1 chance in 16 of doing as well by coin flipping. Our most plausible estimate is based on the fact that, whereas indices of the Southern Oscillation can be highly correlated for many months, the months preceding April of a given year correlate poorly with months following it⁴¹. This suggests treating the first October, January and April of a set as one forecast, independent of a second forecast derived from the subsequent July, October and January. There are now eight independent forecasts, the last seven of which are correct. The probability of guessing this successfully is ~ 0.04 .

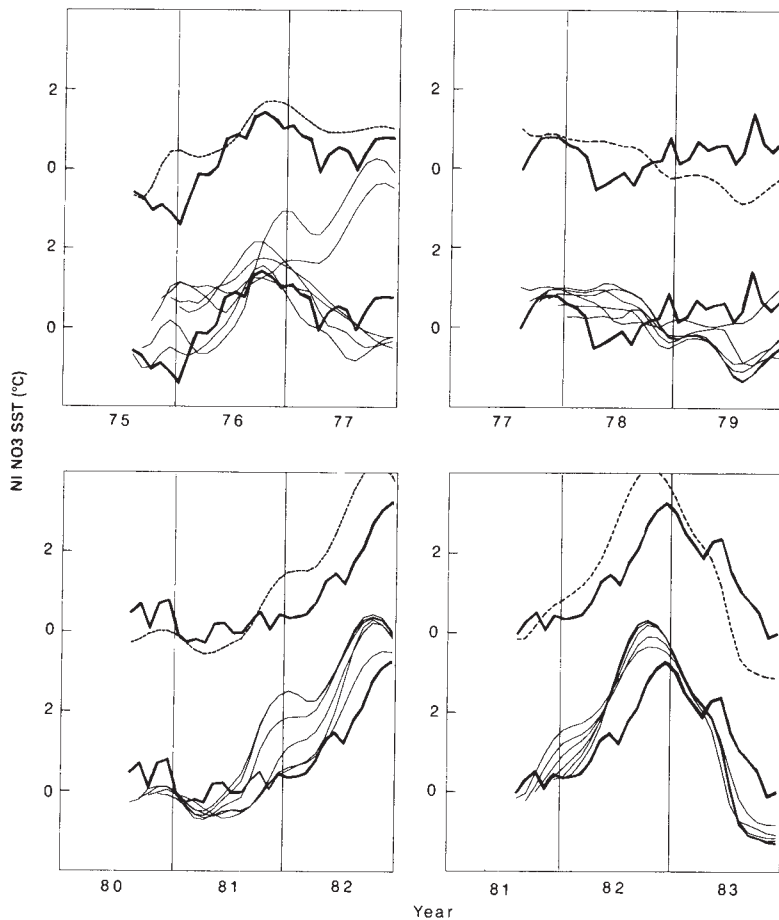


Fig. 3 SST anomalies ($^{\circ}\text{C}$) for selected periods, averaged over the NINO3 region. Light curves, values from forecasts initiated in the six successive months from August to the following January. Dashed curve, average of the six (the consensus forecast); heavy curves, observed values (note repetition of vertical scale).

Another measure of model performance is obtained by considering events and non-events separately. Altogether, 14 of 18 occurrences of El Niño and 5 of 6 non-occurrences are forecast correctly. The joint probability of getting at least that many of each type right by an optimal random strategy is 0.004. (The optimal random strategy assumes *a priori* knowledge of the number of events and non-events in the sample, as well as the score to beat.) The corresponding joint probabilities for the 'conservative' and 'most plausible' cases are 0.06 and 0.04, respectively.

Forecasts started in the same calendar month in different years differ only in their initial conditions. Their success supports the assertion that the future evolution of ENSO is implicit in the initial conditions. Consider, for example, the eight 1-yr forecasts initiated in January. Even if one knew in advance that there were three El Niño events and five non-events, the chance of matching the model performance by guessing all eight correctly is only 1 in 56.

Rather than considering forecasts at 3-month intervals, we now examine a more useful forecasting strategy. A forecast is initiated in each of the 6 successive months from August to January, to obtain the prediction of the ensemble 1 and 2 years ahead. Table 2 summarizes the results of doing this in every year for which we have data (1970–1984), with the exception of the three El Niño years in the sample. A few examples are shown in Fig. 3. There are twelve sets of 1-yr forecasts: in nine of these all 6 months agree so the interpretation of the model prediction is unambiguous. In all nine the prediction is correct. By the rather stringent standard which scores the other three as wrong, the probability of doing as well or better by chance is 0.07.

It would be more accurate to say that the three latter forecasts provide unclear guidance. In two of the cases, where there was no event in the following year, half of the months forecast

correctly and the other half did not. The remaining case is the set from August 1975 to January 1976. As can be seen from Fig. 3, the model actually does a good job of predicting the odd event to come. However, four times out of six our temperature rise criterion is not met because the model SST is too warm at the beginning of 1976. One might quibble with our scoring system, but it would undoubtedly have been difficult to interpret such a forecast at the time.

As might be expected, the 2-yr forecasts are less successful: in five cases all six individual forecasts are correct; in three cases five of six are correct; in the remaining cases one, two or three are correct. Counting eight of the eleven as successes gives

Table 2 Success rates of 6-month sets of forecasts

Forecast from	No. correct (out of 6)	
	1-yr	2-yr
1970	6	5*
1971	6*	1
1973	6	3
1974	6	6*
1975	2*	5
1977	6	6
1978	6	6
1979	6	2
1980	6	6*
1981	6*	6
1983	3	5
1984	3	?

Summary of the sets of forecasts initiated in the six successive months from August to January of each year from 1970 to 1984 (excluding El Niño years). For example, in the first line of the table, the forecasts are from August 1970 to January 1971; the 1-yr forecasts are for 1971 and the 2-yr forecasts are for 1972.

* Year of El Niño event.

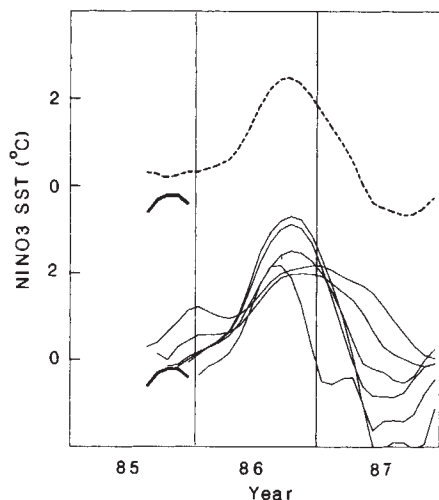


Fig. 4 Forecast for 1986 of SST anomalies ($^{\circ}\text{C}$) in the NINO3 region. Light curves, values from forecasts initiated in the six successive months from August 1985 to January 1986. Dashed curve, average of the six forecasts; heavy curves, observed values (note repetition of vertical scale).

an 89% confidence level. The most consistent failure is the 1971 set, in which all forecasts predicted the 1972 E Niño but five of the six had the warming persist through 1973. Four of the 1979 forecasts predicted an event in 1981, a year early. The 1983 set is the most ambiguous; note that for the years since the outsized 1982 event both the 1- and 2-yr forecasts have been inconsistent.

We present another case, which cannot be evaluated at the time of writing: the prediction for 1986. Figure 4 shows the forecasts initiated in August 1985 to January 1986: all six predict an El Niño event. The amplitude of the consensus forecast suggests it will be a moderate event, not as strong as the events of 1982, 1972 or 1957. However, the only other moderate event in our study was the peculiar 1976 El Niño; experience with the moderate event of 1965 and the even weaker 1969 one might help in interpreting the present case. For the three events in our sample (1972, 1976 and 1982) the consensus overstated the maximum NINO3 SST anomaly amplitude by 30% (more precisely, by 28%, 36% and 28%, respectively). Re-scaling the 1986 forecast accordingly indicates an amplitude of 1.9°C , well below the 3.2°C of 1982 or the 2.5°C of 1972, but above the 1.4°C of 1976.

How much confidence should be placed in the prediction of a 1986 El Niño? As with all forecasting, there exists the possibility that the present case will put pressure on previously untested weak points in the model. Forecasts since the 1982–83 event have been problematical in some respects, possibly reflecting a shift in circulation regime which could adversely affect model performance. Although all of the 1985 forecasts predict an event for 1986, none of the 2-yr forecasts from 1984 predicts it. This is unprecedented among the limited set of cases we have studied. Also, both the 1983 and 1984 1-yr forecasts lack the consistency which is typical of earlier years. Nonetheless, in no previous case in which all six 1-yr forecasts agreed were they incorrect. Moreover, all eleven forecasts from March 1985 to January 1986 give the same result.

Discussion

The ability of the model to predict at long lead times lends support to the theory outlined above⁵, especially the idea that the ENSO cycle owes its existence to interactions in the tropical Pacific. Although the thermal anomalies in the upper layers of the tropical ocean are crucial to the long timescale of the cycle, the ocean alone could not sustain the cycle from event to event. It is an essential part of the ENSO cycle that the two-way coupling between tropical atmosphere and ocean is active in

both the El Niño and non-El Niño phases of the cycle.

The results presented here have significant implications for the future prospects of ENSO prediction systems. It seems clear that the predictability limit for ENSO is years rather than weeks or months. We cannot yet state it more precisely, and it cannot be calculated from forecasts alone because the intrinsic lack of predictability of the coupled ocean–atmosphere system is not the only reason for inaccurate forecasts; poor data and model errors also contribute. We presume these failings account for the cases where the forecasts from many consecutive months are both consistent and wrong (for example, the forecasts for 1973 from 1971). It is also likely that the predictability is highly variable: at some times the future evolution of the coupled system is insensitive to small changes; at others, the system passes so close to a bifurcation point that even small-amplitude disturbances may alter its future behaviour substantially, perhaps making the difference between El Niño and non-El Niño states. We conjecture that the latter times are those for which forecasts from consecutive months are inconsistent (for example, the forecasts from 1983). Here we are implicitly assuming that month-to-month variations in initial conditions are sufficient to reveal all of these uncertain times. Further studies may reveal a better indicator of periods of unpredictability.

In view of the sparsity of the observations used to produce model initial conditions, the success of the forecasts is somewhat surprising, and certainly encouraging. Even without any new breakthroughs in understanding, it should be possible to lengthen the lead time of the model predictions, increase their reliability and improve the forecast of features more subtle than NINO3 SST.

Much more could be done to process the initial data for the purpose of forecasting. All operational meteorological forecast models have very elaborate procedures for data assimilation and model initialization. The only observations used here are ship reports of surface winds. Available observations of SST, currents and ocean thermal structure should be incorporated in the initial fields. Enhancement of the observing system would increase forecast skill: we expect remote sensing of surface winds from satellites to be especially beneficial.

The model used here was developed for theoretical studies, rather than forecasting. It was deliberately simplified in order to isolate the physics believed to be essential to ENSO, putting it at a level of complexity comparable to numerical weather prediction models of 30 years ago. Because our model is based on physical principles, it can be elaborated to increase the fidelity of its simulations. It seems clear that with better observing networks and more refined models, operational climate forecasts of definite social and economic benefit can be expected in the near future.

We dedicate this paper to the memory of Dr Adrian Gill in appreciation of the encouragement he gave this work, and, more broadly, in recognition of his essential contributions to the understanding of ENSO. We thank Professor J. J. O'Brien and David Legler of Florida State University for providing the surface wind analysis, Dr George Philander for his stimulating comments on an earlier draft, and Professor Harold Sackowitz for advice on statistical matters. This work was supported by grants NA-84-AA-D-0031 from the US TOGA Office of NOAA, NA-84-RAD-05082 from EPOCS/NOAA, and NAGW-582 from NASA. This is Lamont–Doherty Geological Observatory contribution 4004.

Note added in proof: No indication of El Niño is apparent as of the end of May 1986. There is no known precedent for an event to begin later than June.

Received 10 March; accepted 8 May 1986.

1. Cane, M. A. *Science* **222**, 1189–1194 (1983).
2. Rasmusson, E. M. & Wallace, J. M. *Science* **222**, 1195–1202 (1983).
3. Rasmusson, E. M. *Am. Sci.* **73**, 168–177 (1985).
4. Gill, A. E. & Rasmusson, E. M. *Nature* **305**, 229–234 (1983).

5. Philander, S. G. H. *Nature* **302**, 215–301 (1983).
6. Canby, T. Y. *Natn. geogr. Mag.* **165**, 144–183 (1983).
7. Glantz, M. H. *Oceanus* **27**, 14–19 (1984).
8. Barnett, T. P. *Mon. Weath. Rev.* **111**, 756–773 (1983).
9. Inoue, I. & O'Brien, J. J. *Mon. Weath. Rev.* **112**, 2326–2337 (1984).
10. Zebiak, S. E. & Cane, M. A. *Mon. Weath. Rev.* (in the press).
11. Cane, M. A. & Zebiak, S. E. *Science* **228**, 1085–1087 (1985).
12. Lau, K.-M. & Chan, P. *Mon. Weath. Rev.* **113**, 1889–1909 (1985).
13. Bjerknes, J. *Mon. Weath. Rev.* **97**, 163–172 (1969).
14. Cane, M. A. *Rev. Earth planet. Sci.* **14**, 43–70 (1986).
15. Wyrski, K. *J. phys. Oceanogr.* **5**, 572–584 (1975).
16. Wyrski, K. *J. phys. Oceanogr.* **9**, 1223–1231 (1979).
17. Busalacchi, A. J. & O'Brien, J. J. *J. geophys. Res.* **86**, 10901–10907 (1981).
18. Gill, A. E. *J. phys. Oceanogr.* **13**, 586–606 (1983).
19. Harrison, D. E. & Schopf, P. S. *Mon. Weath. Rev.* **112**, 923–933 (1984).
20. Zebiak, S. E. & Cane, M. A. *J. phys. Oceanogr.* (submitted).
21. Ramag, C. S. & Hori, A. M. *Mon. Weath. Rev.* **109**, 1827–1835 (1981).
22. Lau, N.-C. *Mon. Weath. Rev.* **113**, 1970–1996 (1985).
23. Shukla, J. & Wallace, J. M. *J. Atmos. Sci.* **40**, 1613–1630 (1983).
24. Boer, G. J. in *Coupled Ocean-Atmosphere Models* (ed. Nihoul, J.) 7–18 (Elsevier, Amsterdam, 1985).
25. Gill, A. E. *Q. J. R. met. Soc.* **106**, 447–462 (1980).
26. Webster, P. J. *J. Atmos. Sci.* **38**, 554–571 (1981).
27. Zebiak, S. E. *J. Atmos. Sci.* **39**, 2017–2027 (1982).
28. Zebiak, S. E. *Mon. Weath. Rev.* (in the press).
29. McCreary, J. P. *Mon. Weath. Rev.* **111**, 370–389 (1983).
30. Anderson, D. L. T. & McCreary, J. P. *J. Atmos. Sci.* **42**, 615–628 (1985).
31. Philander, S. G. H., Yamagata, T. & Pacanowski, R. C. *J. Atmos. Sci.* **41**, 604–613 (1984).
32. Hirst, A. *J. Atmos. Sci.* (in the press).
33. Lau, K.-M. *J. Atmos. Sci.* **38**, 248–261 (1981).
34. McCreary, J. P. *Rev. Fluid. Mech.* **17**, 359–409 (1985).
35. Cane, M. A. & Sarachik, E. S. *J. mar. Res.* **35**, 395–432 (1977).
36. Wyrski, K. *J. geophys. Res.* **90**, 11719–11725 (1985).
37. Lau, K.-M. *J. Atmos. Sci.* **42**, 1552–1558 (1985).
38. Vallis, G. K. *Science* **232**, 243–245 (1986).
39. White, W. & Pagan, S. *J. phys. Oceanogr.* (submitted).
40. Goldenbert, S. B. & O'Brien, J. J. *Mon. Weath. Rev.* **109**, 1190–1207 (1981).
41. Wright, P. *Bull. Am. met. Soc.* **66**, 398–412 (1985).

Secular variation in carbon isotope ratios from Upper Proterozoic successions of Svalbard and East Greenland

A. H. Knoll*, J. M. Hayes†, A. J. Kaufman†, K. Swett‡ & I. B. Lambert§

* Department of Organismic and Evolutionary Biology, Harvard University, Cambridge, Massachusetts 02138, USA

† Biogeochemical Laboratories, Department of Chemistry and Geology, Indiana University, Bloomington, Indiana 47405–5101, USA

‡ Department of Geology, University of Iowa, Iowa City, Iowa 52242, USA

§ Baas Becking Geobiological Laboratory, PO Box 378, Canberra ACT 2601, Australia

Analyses of stratigraphically continuous suites of samples from Upper Proterozoic sedimentary successions of East Greenland, Spitsbergen and Nordaustlandet (Svalbard) provide an approximation to the secular variation in carbon isotope ratios during a geologically and biologically important period of change from around 900 million years ago to the beginning of the Cambrian period. Late Riphean carbonates and organic material show a stratigraphically useful pattern of enrichment in ¹³C relative to Phanerozoic or earlier Proterozoic samples. Isotopic compositions of isolated samples from other localities are consistent with a worldwide extended interval of enhanced organic burial and consequent net survival of oxidized material, probably O₂, just before the initial radiation of metazoans.

SECULAR variations in the carbon isotopic composition of sedimentary carbonates and organic materials have been determined with reasonable temporal precision for most of the Phanerozoic eon, and these data have assumed a significant role in discussion of Phanerozoic environmental history^{1–4}. Analyses of Precambrian samples show that on a gross scale the earlier record of carbon isotopic variation is not dissimilar to that of the past 570 Myr (ref. 5); however, insufficient sampling density and a lack of stratigraphic control have hindered attempts to continue the curve representing of carbon isotopic abundances in marine carbonates backward into the Proterozoic.

We report here the results of carbon isotopic analyses of stratigraphically continuous suites of samples collected from Upper Proterozoic sedimentary successions in Nordaustlandet (Svalbard), northeastern Spitsbergen and central East Greenland. Stratigraphic position, palaeoenvironmental setting and petrography have been determined for each sample, and a degree of biostratigraphic control is provided by acritarch assemblages that occur in all three sequences. The sections, which represent widely separated localities within a single sedimentary basin, show smoothly covariant carbon isotope records for both carbonate and organic carbon. Here we consider three questions bearing on the interpretation and significance of these isotopic variations:

(1) Are they primary (that is, reflective of changes in the isotopic composition of carbon available for biosynthesis of organic matter)?

(2) Are they of global extent (representative of changes in

the isotopic composition of oxidized carbon in the world ocean)?

(3) Do they reflect changes in the Earth's surface environment, especially changes in O₂ concentration, which may have been important in late Proterozoic biological evolution?

Geological setting

The close lithostratigraphic similarities between the Upper Proterozoic and Lower Palaeozoic sequences of the East Greenland Caledonides and eastern Svalbard have long been appreciated⁶. The Spitsbergen, Nordaustlandet and East Greenland sections each contain 7,000–8,000 m of unmetamorphosed, predominantly shallow marine sedimentary rocks, comprising two quartz-arenite-carbonate successions separated by an interval of glaciogenic sedimentation^{7–14}. Table 1 summarizes the nomenclature of the sampled rock units, and stratigraphic columns are shown in Fig. 1.

Thick sequences of cross-bedded and rippled sandstones with interbedded rippled, often carbonaceous shales grade upward into carbonates with minor siliciclastic intercalations. The limestone and dolostone successions contain abundant stromatolites, cross-bedded oolites and pisolites, and intraformational conglomerates, all of which indicate intertidal to shallow subtidal marine deposition. The carbonates are overlain abruptly by a diamictite-bearing siliciclastic sequence, which is in turn overlain by a quartz-arenite-carbonate sequence of Cambro-Ordovician age. Microfossil assemblages^{15–17} and stromatolites¹⁸ indicate that the earlier siliciclastic and carbonate sequence was deposited ~900–700 Myr ago, during the late Riphean interval,